

Schiff Bases as Anticorrosive Additives for Mild Steel Corrosion in Acid Media

M.Abirami, S.Sasikala, S.Chitra, K.Parameswari, and A.Selvaraj^{1,†}

Dept. of Chemistry, P.S.G.R.Krishnammal College for Women, Coimbatore, Tamilnadu, India.

¹Dept of Chemistry, CBM College, Coimbatore, Tamilnadu, India.

The influence of Schiff bases on the corrosion inhibition of mild steel in 1 M H₂SO₄ have been investigated by weight loss, gasometry, impedance and polarization techniques. The results obtained reveal that these compounds act as good inhibitors. The inhibition efficiency of Schiff bases increased with concentration and synergistically increased on addition of chromate, sulphate and halide ions. Potentiodynamic polarization measurements clearly reveal that the investigated inhibitors are of mixed type but they are more cathodic in nature. The adsorption of these compounds on mild steel surface for both the acids were found to obey Langmuir adsorption isotherm. The surface morphology was studied by SEM and UV reflectance spectra.

Keywords : corrosion inhibitor, isatin, schiff bases, synergistic inhibition, langmuir adsorption isotherm.

1. Introduction

The use of inhibitors is one of the most practical methods for protection against corrosion, especially in acidic media.¹⁾ Acid solutions are generally used for the removal of rust and scale in several industrial processes. Inhibitors are generally used in the processes to control the metal dissolution. Organic inhibitors are widely used in various industries. Among them, heterocyclic compounds comprise a potential class of inhibitors. There is a wide consideration in the literature regarding corrosion inhibition studies by nitrogen containing heterocyclics.²⁾⁻⁹⁾ The aim of the present work is to evaluate the inhibition efficiency of synthesized Schiff bases, containing nitrogen and oxygen heteroatoms as corrosion inhibitors for mild steel in 1 M H₂SO₄ by weight loss, gasometry and electrochemical methods.

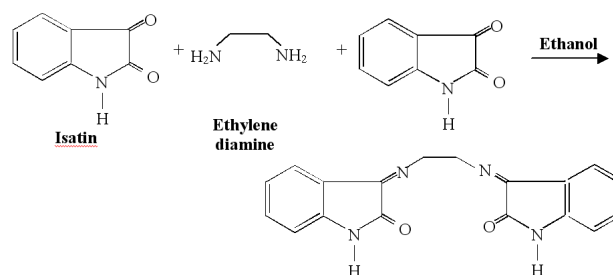
1.1 Experimental methods

Mild steel strips containing C = 0.084 %, P = 0.025%, Mn = 0.369%, S = 0.027% and the remainder iron were used for the measurement of weight loss and gasometric studies. The strips were mechanically polished and degreased with trichloroethylene before use. For electrochemical methods, a cylindrical mild steel rod embedded in Teflon with an exposed area of 0.78 cm² was used. The electrode was polished using a sequence of emery

papers of different grades and then degreased with trichloroethylene. All the chemicals used for the synthesis of the inhibitors were of analar grade.

1.2 Synthesis of the inhibitors

0.2 M of isatin in 50 ml ethanol and 0.1 M of diamine in 25 ml ethanol were mixed and refluxed on steam bath for about two hours and then concentrated in vacuum. The precipitated Schiff base was washed with ethanol and recrystallised from chloroform.¹⁰⁾



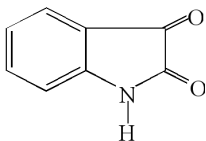
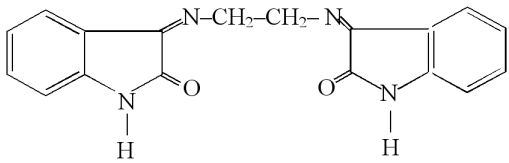
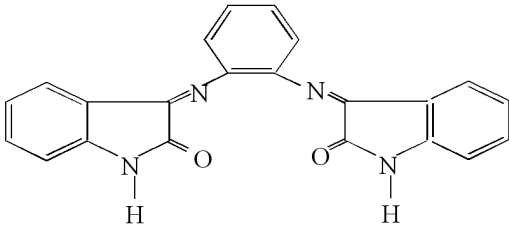
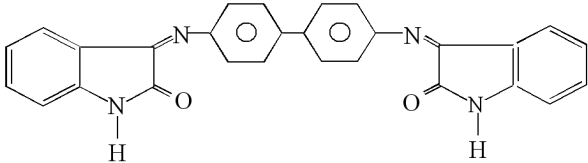
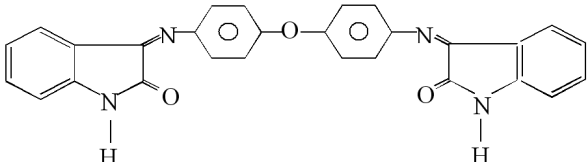
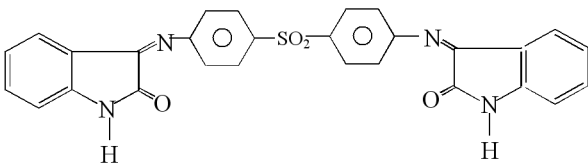
Similarly, three Schiff bases were synthesized using different diamines like benzidine, 4,4'-diamino diphenyl ether and 4,4'-diaminodiphenyl sulphone (Table 1).

1.3 Weight loss method

Mild steel specimens of size 5 cm x 2.5 cm x 0.05 cm were used for weight loss method. The mild steel specimens were polished with emery papers of 1/0 to 4/0 grades

[†] Corresponding author: rajshree1995@rediffmail.com

Table 1.

Structure of the compounds
 <p>Isatin (I)</p>
 <p>Ethylenediamine-bis(isatin) (EnBI)</p>
 <p>o-phenylenediamine-bis(isatin) (PDBI)</p>
 <p>Benzidine-bis(isatin) (BBI)</p>
 <p>4,4-(diaminodiphenylether)-bis(isatin) (DPEBI)</p>
 <p>4,4-(diaminodiphenylsulphone)-bis(isatin) (DPSBI)</p>

and degreased with trichloroethylene. The specimens were hanged into the experimental solution with the help of glass hooks. The experimental solutions (200 ml) contained 1 M H₂SO₄ and different concentrations of the inhibitors. The initial weights of the specimens were noted and were completely immersed into the experimental solu-

tion. After three hours the specimens were taken out, washed thoroughly with distilled water, dried completely and their final weights were noted. Inhibition efficiency (IE), corrosion rate and surface coverage (θ) were calculated using the following equations.

$$\text{Inhibition efficiency} = \frac{(W_0 - W)}{W_0} \times 100$$

Where, W_0 and W are the weight losses in the absence and presence of inhibitors respectively.

$$\text{Corrosion rate (mpy)} = \frac{534 \times W}{A \times T \times D}$$

Where,

A is area of specimen (square inches)

T is exposure of time (h)

D is density of specimen (g/cm³)

W is weight loss (mgm)

$$\text{Surface coverage } (\theta) = \frac{(W_0 - W)}{W}$$

The weight loss method was repeated at higher temperatures from 313 to 333 K at a concentration of 5 mM of inhibitors.

1.4 Gasometric method

Polished and degreased mild steel specimens were suspended from the hook of the stopper and were introduced into the cell containing 200 ml of 1 M H₂SO₄. The same procedure was repeated with 1 M H₂SO₄ containing various concentrations of the inhibitors. From the volume of hydrogen gas liberated, the inhibition efficiency was calculated using the formula.

$$\text{Inhibition efficiency (\%)} = \frac{V_B - V_I}{V_B} \times 100$$

Where,

V_B & V_I are volume of H₂ evolved in the absence and presence of inhibitors.

1.5 Electrochemical studies

1.5.1 Potentiodynamic polarization and impedance measurements

The cells assembly consisted of mild steel as working electrode, platinum as the counter electrode and a saturated calomel electrode (SCE) as the reference electrode. Electrochemical impedance spectral measurements and Tafel

polarization studies were conducted using an electrochemical measurement unit (model 1280B Solartron). Both anodic and cathodic polarization curves were recorded in the absence and presence of inhibitors. Impedance measurements (EIS) were made at corrosion potentials over a frequency range of 10 KHz to 1 MHz with a super imposed sine wave of amplitude 10 mV. The real Z' and imaginary Z'' parts were measured at various frequencies. From the plot of Z' Vs Z'' the charge transfer resistance (R_t) and the double layer capacitance (C_{dl}) were calculated. Impedance measurements were carried out both in the absence and presence of inhibitors at selected concentrations. The inhibition efficiency was calculated using the following equation.

$$\text{Inhibition efficiency (\%)} = \frac{R_t^* - R_t}{R_t^*} \times 100$$

Where, R_t and R_t^* are the charge transfer resistance obtained in the absence and presence of the inhibitors.

After EIS measurements the polarization measurements were carried out at a potential range of -200 mV to +200 mV with respect to open circuit potential at a scan rate of 1 mV/sec.

$$\text{Inhibition efficiency (\%)} = \frac{I_{\text{corr(blank)}} - I_{\text{corr(inh)}}}{I_{\text{corr(blank)}}} \times 100$$

Where, $I_{\text{corr(blank)}}$ and $I_{\text{corr(inh)}}$ are the corrosion current in the absence and presence of inhibitors.

1.6 Atomic absorption spectrophotometric studies

Atomic absorption spectrophotometer (model GBC 908, Australia) was used for estimating the amount of dissolved iron in the corrodent solution containing various concentrations of the inhibitors in 1 M H_2SO_4 after exposing the mild steel specimen for three hours. From the amount of dissolved iron, the inhibition efficiency was calculated.

$$\text{Inhibition efficiency (\%)} = \frac{B - A}{B} \times 100$$

Where,

A and B are the amount of dissolved iron in the presence and absence of the inhibitors.

1.7 Synergistic effect

The synergistic effect was studied by the addition of 1 mM KI to the mild steel specimen immersed in 1 M H_2SO_4 containing various concentrations of the inhibitors for a duration of three hours. From the weight loss data

the corrosion rate and inhibition efficiency was calculated. The same procedure was repeated by the addition of 1 mM KCl, 1 mM KBr, 1 mM K_2CrO_4 and 1 mM K_2SO_4 .

1.8 Surface examination studies

Surface examination of mild steel specimens were made by using scanning electron microscope (SEM) in order to understand the surface morphology of the mild steel in 1 M H_2SO_4 in the presence and absence of inhibitors. The surface morphology was taken using JEOL scanning electron microscope.

1.9 UV reflectance spectral studies

Reflectance studies support the formation of a film on the metal surface that inhibit the corrosion of mild steel in acidic solution in presence of organic compounds. UV visible NIR spectrophotometer in the range 200-700 nm at a normal incident angle of 90° was used. The UV reflectance spectrum was recorded for the surface of polished, corroded and corrosion inhibited mild steel specimens.

2. Results and discussion

2.1 Weight loss measurements

Table 2 shows the values of inhibition efficiency obtained from weight loss measurements for different concentrations of the inhibitors in 1 M H_2SO_4 . In all the Schiff bases the inhibition efficiencies were between 77-92% at 5 mM concentration of the inhibitor. Moreover, the inhibition efficiency was found to increase with increase in inhibitor concentration. A plot of inhibition efficiency against various concentration of the inhibitors is shown in Fig. 1. The order of inhibition efficiency of the tested compounds is

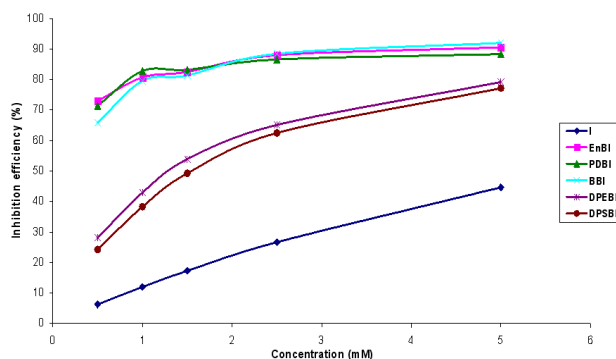


Fig. 1. Plot of inhibition efficiency(%) vs concentration(mM) for the inhibition of corrosion of mild steel in 1 M H_2SO_4

Table 2. Inhibition efficiencies of various concentration of the inhibitors for the corrosion of mild steel in 1 M H₂SO₄ obtained by weight loss measurement at 30±1 °C

Name of the inhibitor	Inhibitor concentration (mM)	Weight loss (gms)	Inhibition efficiency (%)	Corrosion rate (mpy)	Degree of coverage (Θ)
I	Blank	0.5890	-	8990.82	-
	0.5	0.5853	6.28	8934.34	0.0628
	1.0	0.5183	12.00	7911.62	0.1200
	1.5	0.4872	17.28	7436.89	0.1728
	2.5	0.4320	26.66	6594.29	0.2666
	5.0	0.3260	44.65	4976.24	0.4465
EnBI	Blank	0.4578	-	6988.11	-
	0.5	0.1237	72.98	1888.22	0.7298
	1.0	0.0885	80.67	1350.91	0.8067
	1.5	0.0801	82.50	1222.69	0.8250
	2.5	0.0550	87.99	839.55	0.8799
	5.0	0.0433	90.54	660.96	0.9054
PDBI	Blank	0.5324	-	8126.85	-
	0.5	0.1523	71.39	2324.79	0.7139
	1.0	0.0916	82.79	1398.23	0.8279
	1.5	0.0893	83.23	1363.12	0.8323
	2.5	0.0714	86.59	1089.89	0.8659
	5.0	0.0622	88.32	949.46	0.8832
BBI	Blank	0.5324	-	8126.85	-
	0.5	0.1817	65.87	2773.57	0.6587
	1.0	0.1089	79.54	1662.31	0.7954
	1.5	0.0994	81.33	1517.30	0.8133
	2.5	0.0615	88.45	938.77	0.8845
	5.0	0.0425	92.02	648.74	0.9202
DPEBI	Blank	0.5120	-	7815.45	-
	0.5	0.3679	28.14	5615.83	0.2814
	1.0	0.2920	42.97	4457.25	0.4297
	1.5	0.2362	53.87	3605.49	0.5387
	2.5	0.1787	65.10	2727.78	0.6510
	5.0	0.1066	79.18	1627.20	0.7918
DPSBI	Blank	0.5120	-	7815.45	-
	0.5	0.3877	24.28	5918.07	0.2428
	1.0	0.3159	38.30	4822.07	0.3830
	1.5	0.2599	49.24	3967.26	0.4924
	2.5	0.1920	62.50	2930.79	0.6250
	5.0	0.1169	77.17	1784.43	0.7717

The inhibition behaviour of Schiff bases can be explained on the basis of the concept of adsorption of inhibitors on the corroding metal surface. The mechanism of adsorption responsible for the corrosion inhibition for the set of aromatic Schiff bases employed in the present investigation can be derived as follows. The inhibitors contain two to four aromatic rings, two >C=N - groups -NH group and two >C=O groups. Hence they are expected to have adsorbed on the metal surface through the combination of two adsorption mechanism.

1. Interaction of unshared electron pairs on the nitrogen atom (Fig. A)

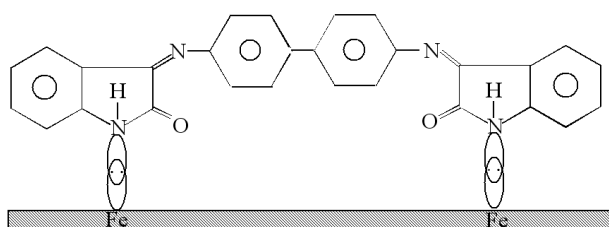


Figure-A

2. Interaction of π -electrons of the aromatic ring and >C=N - group with the metal surface (Fig. B)

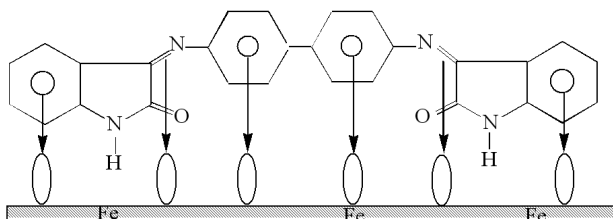


Figure-B

The above interactions are facilitated by the flat orientation of the molecule with respect to the metal surface. Both the mechanism must have contributed to the adsorption of the dianils on the metal surface. The order of inhibition efficiency of the tested compounds is



The compound (I) has the lowest inhibition efficiency of 44% at 5 mM concentration in comparison to the other compounds. This may be due to the presence of one benzene ring, one >NH and two >C=O groups in comparison to 3-4 aromatic rings, -NH group two >C=N - groups in the other compounds. Since the number of anchoring sites in isatin is less the extent to which it gets adsorbed on the metal surface is less and this accounts for its minimum inhibition efficiency. The maximum inhibition efficiency of BBI is due to the presence of more anchoring sites namely four benzene rings, two >C=N - group, one -NH group and two >C=O groups. 92% inhibition efficiency of BBI at 5 mM concentration is probably due to the flat orientation of the benzene rings on the mild steel surface providing it a greater degree of protection. On this basis, compounds DPEBI & DPSBI is also expected to have very high inhibition efficiency. But their inhibition efficiency values are only 79% and 77% respectively. The reason for the low inhibition efficiency of DPEBI and DPSBI in comparison to BBI was derived from the IR spectra of the corrosion product obtained by scraping the film on the mild steel plate by a glass knife after immersion of the plates for 3 hrs in 1 M H_2SO_4 containing 5 mM DPEBI & DPSBI respectively. In the case of IR spectra of the corrosion product of DPEBI peaks at 3766.7 cm^{-1} and 3415.7 cm^{-1} characteristics of -OH stretching was observed. Similarly in the IR spectra of the corrosion product of DPSBI peaks at 2330 cm^{-1} & 2360 cm^{-1} characteristic of -OH stretching was observed. The appearance of these bands may probably be due to the reduction of C-O-C group to -C-OH in DPEBI and -SO_2 - group to -SH in DPSBI by the hydrogen evolved at the surface

of the electrode. Hence it can be concluded that the lower absorbability of DPEBI & DPSBI may be due to their decomposition to -OH and -SH compounds which has a lesser tendency to adsorb on the metal surface.^{11,12)}

The dianil PDBI has slightly lower inhibition efficiency in comparison to BBI. This may be attributed to orientation of the benzene ring of the diamine. Probably this benzene ring does not act as an anchoring site for the adsorption process as it is expected to be oriented perpendicular to the adsorption plane, preventing flat orientation of the molecule on the metal surface.¹³⁾

Grigorev et al.,¹⁴⁾ and Pullevits¹⁵⁾ have found that the increase of alkyl chain length has increased the absorbability of the inhibitor molecule. Hackerman et al.,¹⁶⁾ have noted that inhibitors with increasing alkyl chain length form a widely spread film and thereby prevent corrosion better than those with lower molecular weight. Thus the fact that the compound EnBI has higher inhibition efficiency can be substantiated based on the above review.

2.2 Effect of temperature

The values of inhibition efficiency at 5 mM concentration of the inhibitors for the corrosion inhibition of mild steel in 1 M H_2SO_4 solution at different temperatures ranging from 303-333°K are given in Table 3. It can be seen that inhibition efficiency decreased with increase in temperature. Arrhenius plots (log corrosion rate Vs $1/T$) shown in Fig. 3 were used for the calculation of activation energies. The values of E_a in the inhibited acid solutions are appreciably greater than those obtained in the uninhibited acid solution. This suggests that presence of reactive centres on the inhibitors block the active sites for corrosion resulting in an increase in activation energy.

The free energy of adsorption ($\Delta G_{\text{ads}}^{\circ}$) at various temperatures was calculated using the relation.

$$\Delta G_{\text{ads}}^{\circ} = -RT \ln(55.5K)$$

$$\text{and } k \text{ is given by } = \frac{\theta}{C(1-\theta)}$$

Table 3. Inhibition efficiencies at 10 mM concentration of inhibitors for the corrosion of mild steel in 1 M H_2SO_4 obtained by weight loss measurements at higher temperatures

Name of the inhibitor	Inhibition efficiency (%)			
	303 °K	313 °K	323 °K	333 °K
I	44.63	35.86	34.34	27.84
EnBI	92.66	88.18	83.51	78.02
PDBI	89.45	85.45	81.86	74.19
BBI	85.63	78.68	71.64	57.06
DPEBI	68.67	59.24	46.67	30.21
DPSBI	80.13	71.24	65.08	53.92

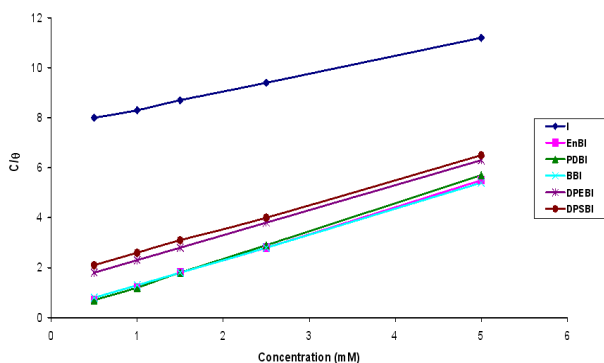


Fig. 2. Langmuir plot of the inhibitors in 1 M H₂SO₄

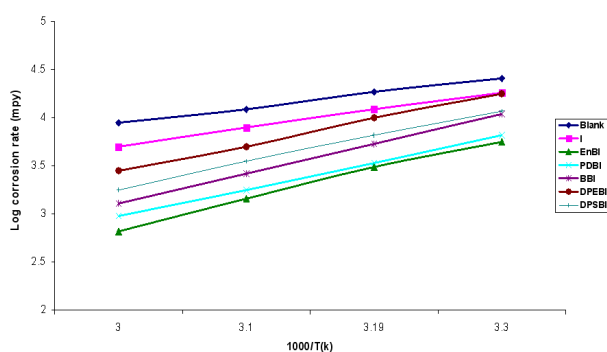


Fig. 3. Arrhenius plot of corrosion rate of mild steel in 1 M H₂SO₄ solution in the absence and presence of inhibitors

Table 4. Activation energies (E_a) and free energy of adsorption (ΔG_{ads}^0) for the corrosion of mild steel in 1 M H₂SO₄ at 5 mM concentration of the inhibitors

S.No	Name of the inhibitor	E_a (kJ)	ΔG_{ads}^0 at various temperatures (kJ)			
			303 k	313 k	323 k	333 k
1.	Blank	26.11	-	-	-	-
2.	I	38.29	-5.52	-4.75	-4.72	-4.03
3.	EnBI	60.92	-12.45	-11.49	-10.82	-10.17
4.	PDBI	52.22	-11.45	-10.87	-10.51	-9.59
5.	BBI	57.44	-10.56	-9.66	-8.95	-7.45
6.	DPEBI	47.87	-8.074	-7.24	-6.11	-4.35
7.	DPSBI	63.82	-9.56	-8.62	-8.14	-7.10

The values of E_a and ΔG_{ads}^0 are given in Table 4. The low and negative values of ΔG_{ads}^0 indicate the spontaneous adsorption of inhibitors on the surface of mild steel.¹⁷⁾

2.3 Nature of adsorption isotherm

Weight loss data were tested graphically for fitting a suitable isotherm. Plot of C/θ Vs C for all the compounds gave a straight line (Fig. 2) proving the fact that the adsorption of these compounds on the mild steel surface obeys Langmuir adsorption isotherm. The adsorption of

the inhibitors on the metal surface may be either physisorption or chemisorption. Though it is not possible to clearly identify the type of adsorption, which type of adsorption predominates over the other can be interpreted based on weight loss data at higher temperatures. From Table 4 it is clear that E_a for inhibited systems are higher than those of uninhibited system. According to Radovic¹⁸⁾ for the inhibitors which involve in predominant physisorption, inhibition efficiency decreases with increase in temperature. Hence although the inhibitors taken for study can interact with mild steel surface through physisorption and chemisorption mechanism, it is the physisorption mechanism which predominates.

2.4 Gasometric method

Table 5 gives the values of inhibition efficiency obtained using the gasometric method for the volume of gas collected in the absence and presence of the inhibitors (I, EnBI and PDBI) at constant temperature of about $30 \pm 1^\circ\text{C}$ for the corrosion of mild steel in 1 M H₂SO₄. The volume of gas collected decreased with addition of inhibitors causing the inhibition efficiency to increase with increase in the concentration of the inhibitor. There is a good agreement between the values of inhibition efficiency obtained from weight loss method and gasometric measurements.

2.5 Electrochemical studies

2.5.1 Potentiodynamic polarization and impedance measurements

2.5.1.1 AC-impedance measurements

The corrosion behaviour of mild steel in acidic solution in the presence and absence of the inhibitors was investigated by EIS method at $30 \pm 1^\circ\text{C}$ after immersion for 10 minutes. The impedance diagrams obtained were perfect semi circles (Fig. 4). The charge transfer resistance, R_t

Table 5. Inhibition efficiencies for the selected concentrations of the inhibitors for the corrosion of mild steel in 1 M H₂SO₄ obtained by gasometric measurement

S.No	Name of the inhibitor	Inhibitor concentration (mM)	Volume of gas (cc)	Inhibition efficiency (%)
1.	I	Blank	26.8	-
		0.5	24.6	8.21
		1.5	21.2	20.96
		5.0	15.8	41.04
2.	EnBI	0.5	7.2	73.13
		1.5	5.2	80.60
		5.0	2.5	90.67
3.	PDBI	0.5	7.4	72.39
		1.5	4.8	82.09
		5.0	2.8	89.55

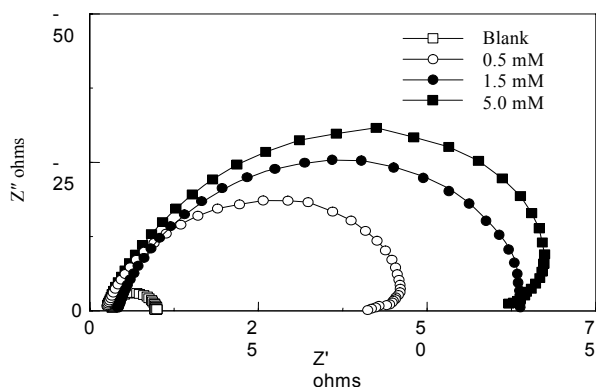


Fig. 4. Nyquist diagram for mild steel in 1 M H₂SO₄ for selected concentrations of inhibitor (PDBI)

Table 6. AC-impedance parameters for mild steel for selected concentrations of the inhibitors in 1 M H₂SO₄

S.No	Name of the inhibitor	Inhibitor concentration (mM)	R _t (ohmcm ²)	C _{dl} (μF/cm ²)	Inhibition efficiency (%)
1.	EnBI	Blank	6.5444	24.5260	-
		0.5	14.4221	18.9440	54.62
		1.5	46.9669	15.0390	86.07
		5.0	138.1300	14.5570	95.26
2.	PDBI	0.5	41.9263	21.5860	84.39
		1.5	61.6375	20.8700	89.38
		5.0	64.7650	19.9190	89.90
3.	BBI	0.5	15.2258	16.5260	57.02
		1.5	40.7366	13.6710	83.93
		5.0	49.5400	10.4300	86.93
4.	DPEBI	0.5	16.8667	22.6660	61.20
		1.5	49.9173	21.3570	86.89
		5.0	52.2536	18.2150	87.48

values were calculated from the difference in impedance at lower and higher frequencies as suggested by Tsuru and Haruyama.¹⁹⁾ To obtain the double layer capacitance(C_{dl}) the frequency at which the imaginary component of the impedance is maximum (-Z'' max) was found and C_{dl} values were obtained from the equation. The data are presented in Table 6.

$$F(-Z'' \text{ max}) = \frac{1}{2\pi C_{dl} R_t}$$

The value of R_t increased with increase in the concentrations of the inhibitor and this in turn leads to increase in inhibition efficiency. As impedance diagrams for solutions examined have almost a semicircular appearance, it indicates that the corrosion of steel is mainly controlled by a charge transfer process. The C_{dl} values decreases, proving the adsorption of Schiff bases on the metal surface leading to the formation of a film.²⁰⁾

2.6 Polarization studies

Both anodic and cathodic polarization curves for mild steel in 1 M H₂SO₄ at selected concentration of the inhibitors are shown in Fig. 5. Values of corrosion current density (I_{corr}), corrosion potential (E_{corr}), tafel slopes (b_a and b_c) and corrosion inhibition efficiency for selected concentrations of the inhibitors are presented in Table 7. It is evident from the table that I_{corr} decreases with increasing inhibitor concentration resulting in an increase in inhibition efficiency. The Tafel constants b_a and b_c are both affected but b_c is affected to a greater extent (fig. 5). Hence it can be concluded that although all the inhibitors behave as mixed type inhibitors they are more cathodic in nature.

Table 7. Corrosion parameters for mild steel with selected concentrations of the inhibitors in 1 M H₂SO₄ by potentiodynamic polarization method

S.No	Name of the inhibitor	Inhibitor concentration (mM)	Tafel slopes (mg/dec)		E _{corr} (mV)	I _{corr} (μAmp/cm ²)	Inhibition efficiency (%)
			b _a	b _c			
1.	EnBI	Blank	154.90	190.20	-445.60	2700.00	-
		0.5	139.60	149.00	-455.40	1340.00	50.37
		1.5	132.40	150.20	-444.00	904.15	66.51
		5.0	113.00	141.00	-463.37	625.18	76.84
2.	PDBI	0.5	135.80	139.00	-448.60	805.49	70.17
		1.5	122.60	153.50	-434.50	562.29	79.17
		5.0	128.80	112.90	-479.40	418.88	84.49
3.	BBI	0.5	129.60	149.00	-451.50	1070.00	60.37
		1.5	129.10	144.00	-453.50	895.48	66.83
		5.0	137.00	147.10	-447.10	816.97	69.74
4.	DPEBI	0.5	123.00	151.00	-455.40	1170.00	56.67
		1.5	135.00	143.00	-444.10	932.67	65.46
		5.0	139.00	142.50	-448.70	858.46	68.21

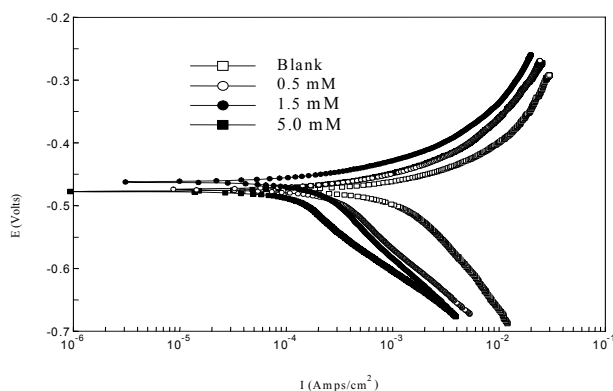


Fig. 5. Polarization curves for mild steel recorded in 1 M H₂SO₄ for selected Concentrations of inhibitor (PDBI)

Table 8. Atomic Absorption Spectroscopy Amount of dissolved iron present in the corrosive solution with and without inhibitors in 1 M H₂SO₄

S.No	Name of the inhibitor	Inhibitor concentration (mM)	Amount of iron content (mg/l)	Inhibition efficiency (%)
1.	EnBI	Blank	2569.5	-
		0.5	677.6	73.63
		5.0	511.5	80.09
2.	DPEBI	0.5	1880.6	29.92
		5.0	521.5	79.70

2.7 Atomic absorption spectrophotometric studies

Percentage inhibition efficiency of the inhibitors (EnBI and DPEBI) towards the dissolution of iron was calculated and the results are given in Table 8. The percentage in-

hibition efficiency obtained by this technique was found to be in good agreement with that obtained from the conventional weight loss method.

2.8 Synergism

The synergistic effect provided by the addition of halide ions, I⁻, Br⁻ and Cl⁻ to the solution containing 1 M H₂SO₄ and the synthesized compounds were studied by weight loss method and the data are presented in Table 9. Analysis of the data revealed that the synergistic influence of halide ions follows the order, I⁻ > Br⁻ > Cl⁻. This observed order suggests that I⁻ has highest synergistic influence among the halide ions.¹⁹⁾ This may be explained as follows:- The steel surface is originally positively charged in 1 M H₂SO₄. When I⁻ ion are added to the inhibiting solution they are strongly chemisorbed by forming chemical bonds even leading to the formation of iron iodide. This strong chemisorption of I⁻ ions shift ϕ_n of the metal to more positive potential than in the case of Cl⁻ and Br⁻ and renders the surface more highly negatively charged. On the highly negatively charged metal surface, the protonated cationic inhibitor molecules are physisorbed due to electrostatic interaction. This interaction, will be higher for I⁻ than for Cl⁻ or Br⁻ due to higher magnitude of negative charge on the metal surface. Hence the observed order is I⁻ > Br⁻ > Cl⁻.

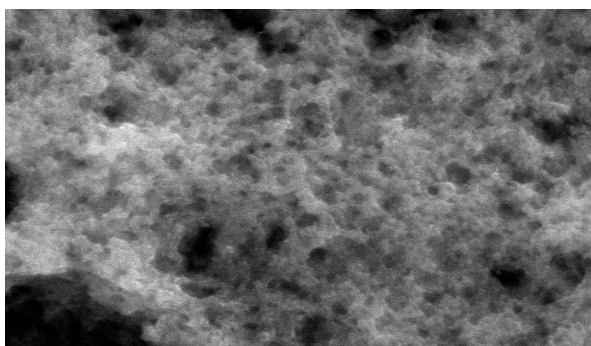
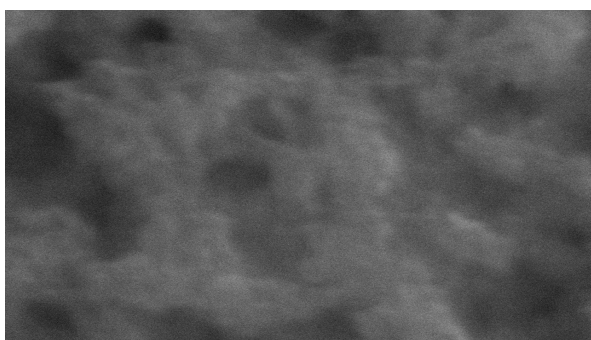
The synergism provided by other anions namely chromate and sulphate was also studied by weight loss method by the addition of 1 mM potassium chromate and sulphate (Table 10). Chromate ions were found to exhibit higher synergism in comparison to sulphate ions.

Table 9. Synergistic effect of 1 mM KCl / 1 mM / KBr / 1 mM KI on the inhibition efficiency of I, EnBI and PDBI by weight loss method at 30±1°C

S.No	Name of the inhibitor	Inhibitor concentration on mM	Inhibition efficiency (%)			
			Without KCl, KBr & KI	With 1mM KCl	With imM KBr	With 1mM KI
1.	I	0.25	6.24	8.36	11.69	14.24
		0.50	6.28	9.42	12.70	15.35
		0.75	6.91	8.28	13.65	17.68
		1.00	11.68	13.58	15.67	20.28
		1.50	20.84	23.46	27.92	30.16
2.	EnBI	0.25	72.98	75.08	77.22	80.95
		0.50	75.29	77.39	80.12	82.46
		0.75	77.70	79.17	81.62	84.28
		1.00	79.66	81.02	83.23	85.52
		1.50	82.50	83.66	85.86	86.46
3.	PDBI	0.25	31.68	33.98	35.58	39.88
		0.50	66.59	69.39	70.02	72.18
		0.75	73.74	75.51	77.65	79.24
		1.00	80.41	83.51	83.51	85.17
		1.50	82.10	83.52	85.63	87.08

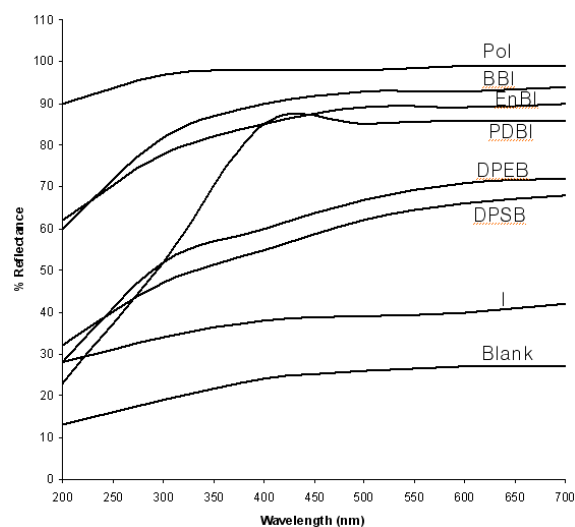
Table 10. Synergistic effect of 1 mM K₂CrO₄ and 1 mM K₂SO₄ on the inhibition efficiency of inhibitors by weight loss method at 30±1 °C

S.No	Name of the inhibitor	Inhibitor concentration (mM)	Inhibition efficiency (%)		
			Without K ₂ CrO ₄ & K ₂ SO ₄	With 1mM K ₂ CrO ₄	With 1mM K ₂ SO ₄
1.	I	0.25	6.24	23.90	12.12
		0.50	6.28	24.36	12.76
		0.75	6.91	26.46	14.52
		1.00	11.68	33.54	29.94
		1.50	20.24	54.82	36.18
2.	EnBI	0.25	72.98	92.75	86.35
		0.50	75.29	94.46	89.52
		0.75	77.70	95.37	91.68
		1.00	79.66	95.76	91.89
		1.50	82.50	97.42	93.88
3.	PDBI	0.25	31.68	61.62	55.76
		0.50	66.59	86.19	70.82
		0.75	73.74	86.24	74.92
		1.00	80.41	89.71	82.18
		1.50	82.10	93.56	84.84

**Fig. 6.** Scanning Electron Microscopy Photographs Blank (1 M H₂SO₄)**Fig. 7.** EnBI (5 mM)

3. SEM

The formation of an adsorbed protective film of the inhibitor molecule on the mild steel surface is also confirmed by SEM studies. Figs. 6 and 7 shows the scanning electron

**Fig. 8.** UV reflectance curves for mild steel specimens under different conditions in 1 M H₂SO₄

micrographs of mild steel specimens exposed to 1 M H₂SO₄ and 1 M H₂SO₄ containing 5 mM concentration of EnBI, uniform corrosion can be observed in Fig. 7. It can be seen in Fig. 7 that the metal surface is fully covered with the inhibitor molecules giving it a high degree of protection.

3.1 UV reflectance studies

The film formation on the metal surface was also supported by reflectance studies for different specimens under similar conditions. Fig. 8 shows the reflectance curve for polished mild steel specimen, specimen dipped in 1 M

H₂SO₄ in the absence and presence of the inhibitors. It can be seen that the reflectance is maximum for the polished specimen and it is brought down considerably in the case of specimens dipped in 1 M H₂SO₄. A close look at the Figs. reveals the fact that the performance of BBI is the best in this regard followed by EnBI, PDBI, DPEBI, DPSBI and I in the decreasing order.

4. Conclusions

- 1) Isatin has very low inhibition efficiency.
- 2) All investigated Schiff bases are effective inhibitors for corrosion of mild steel in 1 M H₂SO₄.
- 3) The inhibition efficiency increases with increase in inhibitor concentration.
- 4) The adsorption of these inhibitors follows Langmuir adsorption isotherm.
- 5) The effect of temperature indicates that the inhibition efficiency decreases with increasing temperature.
- 6) The activation energy (E_a) is higher for inhibited acids than for uninhibited acids showing the temperature dependence of inhibition efficiency.
- 7) The Tafel slopes obtained from potentiodynamic polarization curves indicate that they are cathodic in nature.

References

1. G. Trabanelli, *Corrosion*, **47**, 410 (1991).
2. S. L. Granese, B. M. Rosales, C. Oviedo, and J. O. Zerbino, *Corros. Sci.*, **33**, 1439 (1992).
3. G. Subramaniam, K. Balasubramaniam, and P. Shridhar, *Corros. Sci.*, **30**, 1019 (1990).
4. S. N. Banerjee and S. Mishra, *Corros.*, **45**, 780 (1989).
5. S. Hettiarachi, Y. W. Chain, R. B. Wilson JR, and VS Agarwala, *Corros.*, **45**, 30 (1989).
6. C. R. Anderson and G. M. Schmidt, *Corros. Sci.*, **24**, 325 (1984).
7. E. Stupnisek-Lisac, M. Meticos-Hukovic, D. Lencic, J. Vorkapic-Furac, and K. Berkovic, *Corrosion*, **48**, 924 (1992).
8. E. Stupnisek-Lisac, K-Berkovic, and J. Vorakapic-Furac, *Corros. Sci.*, **12**, 1189 (1988).
9. S. N. Raicheva, B. V. Aleksiev, and E. J. Sokolov, *Corros. Sci.*, **34**, 343 (1993).
10. C. Pamau, A. Kriza, V. Pop, and S. Udrea, *J. of Indian Chem. Soc.*, **82**, 71 (2005).
11. V. S. Komkhadze and S. A. Balezin, *Zh. Obshch. Khim.*, **22**, 848 (1952).
12. G. P.Cicileo, B. M.Rosales, F. E. Vavela, and J. R. Vilche, *Corr. Sci.*, **41**, 1359 (1999).
13. M. A. Quraishi, Mohd Qasim Ansare, Shamum Ahmad, and G. Venkatachari, *Bull. Electrochem.*, **14**, 342 (1998).
14. N. B. Grigorev and D. N. Machavariani, in "The double layer and adsorption on solid electrode (in Russian), *Tartu, Es. SSR.*, **19**, 61 (1968).
15. R. Ya. Pullevits, V. V. Pal'm, and V. E. Past in "Double layer and adsorption on solid electrodes (Russian) Tartu, Est. SSR, **19**, 125 (1968).
16. N. Hackerman and A. C. Mackrides, *Ind. Eng. Chem.*, **47**, 1773 (1955).
17. G. K. Gomma and M. H. Wahdan, *Indian J. Chem. Technol.*, **2**, 5 (1995).
18. Radovici. O, in *Proceedings of the Second European Symposium on Corrosion Inhibitors*, Ferrarr 178, (1964).
19. T. Tsuru, S. Haruyama, Boshoku Gijutsu, *J. Japan Soc. Corr. Eng.*, **27**, 573 (1978).
20. S. Muralidharan, R. Chandrasekar, *Proc. Indian Acad. Sci.*, **112**, 127 (2000).